

Supporting information for

Tailoring the dimensionality of carbon nanostructures as highly electrochemical supports for detection of carcinoembryonic antigen

Yubo Meng^{1,*,#}, Yingpan Song^{2,*,#}, Chuanpan Guo², Bingbing Cui², Hongfei Ji²,
Zongzheng Ma¹

¹*College of Mechanical Engineering, Henan University of Engineering, No.1, Xianghe Road, Longhu Town, Zhengzhou, Henan, 451191, P. R. China.*

²*Henan Provincial Key Laboratory of Surface and Interface Science, Zhengzhou University of Light Industry, No. 136, Science Avenue, Zhengzhou, Henan, 450001, P. R. China.*

*Corresponding author: myb0201@126.com (Y. Meng) or wangpan8624@163.com (Y. Song)

#These authors contributed equally.

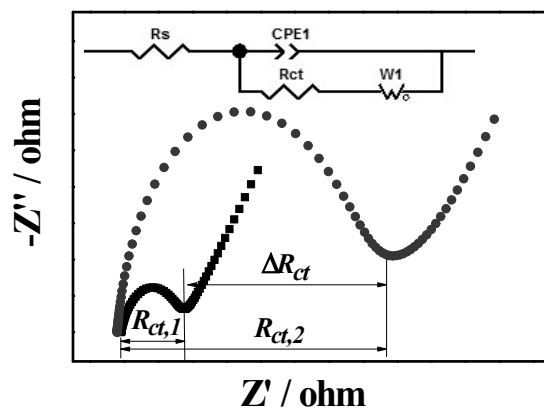


Fig. S1 EIS Nyquist plots and equivalent circuit.

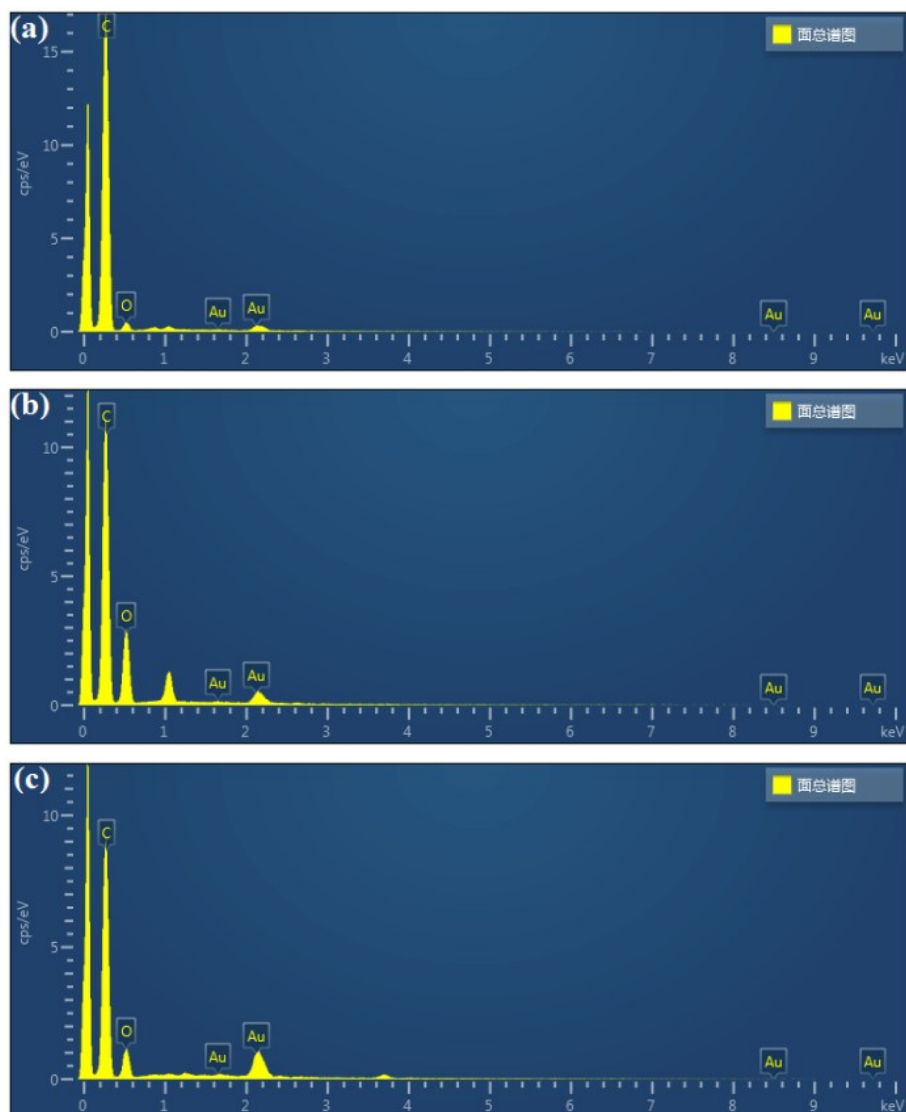


Fig. S2 EDS spectra of the (a) Au/NCNTs, (b) Au/PU-NCNTs, and (c) Au/FU-NCNTs.

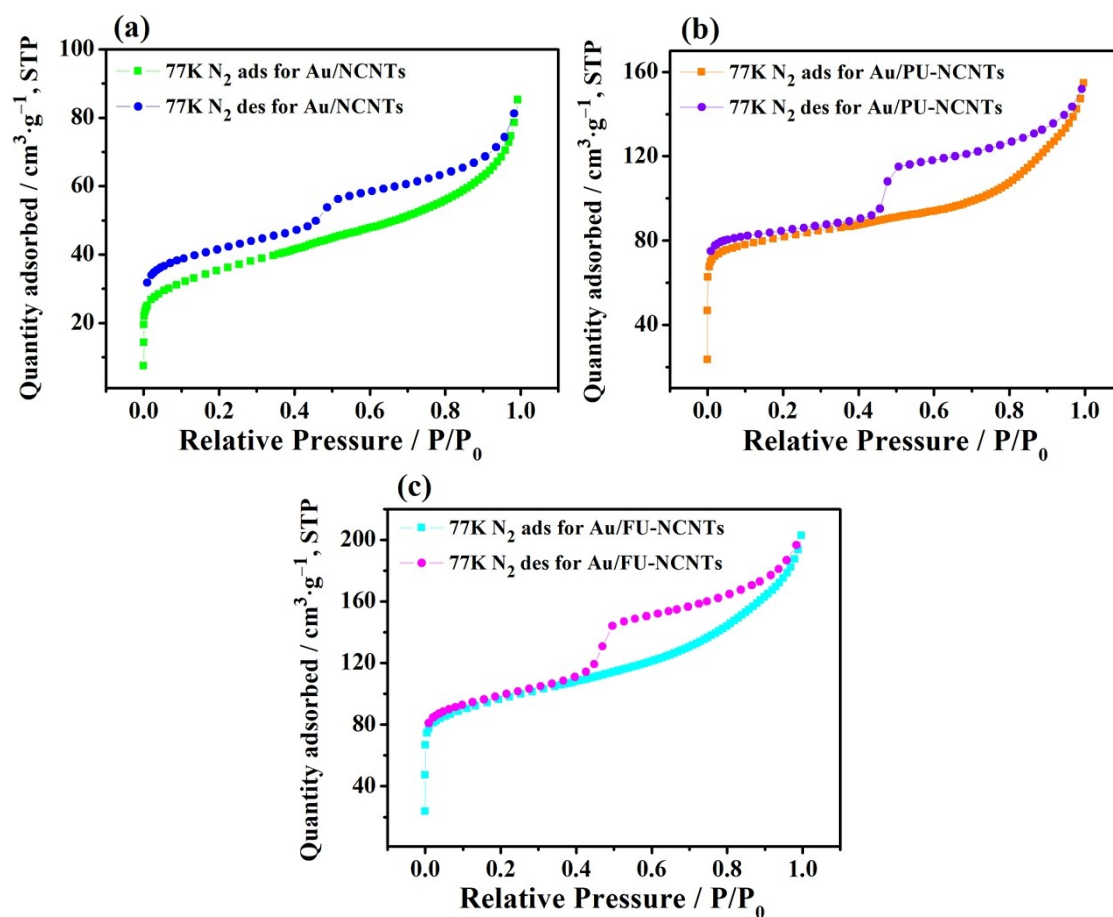


Fig. S3 Nitrogen adsorption–desorption isotherms of (a) Au/NCNTs, (b) Au/PU-NCNTs, and (c) Au/FU-NCNTs.

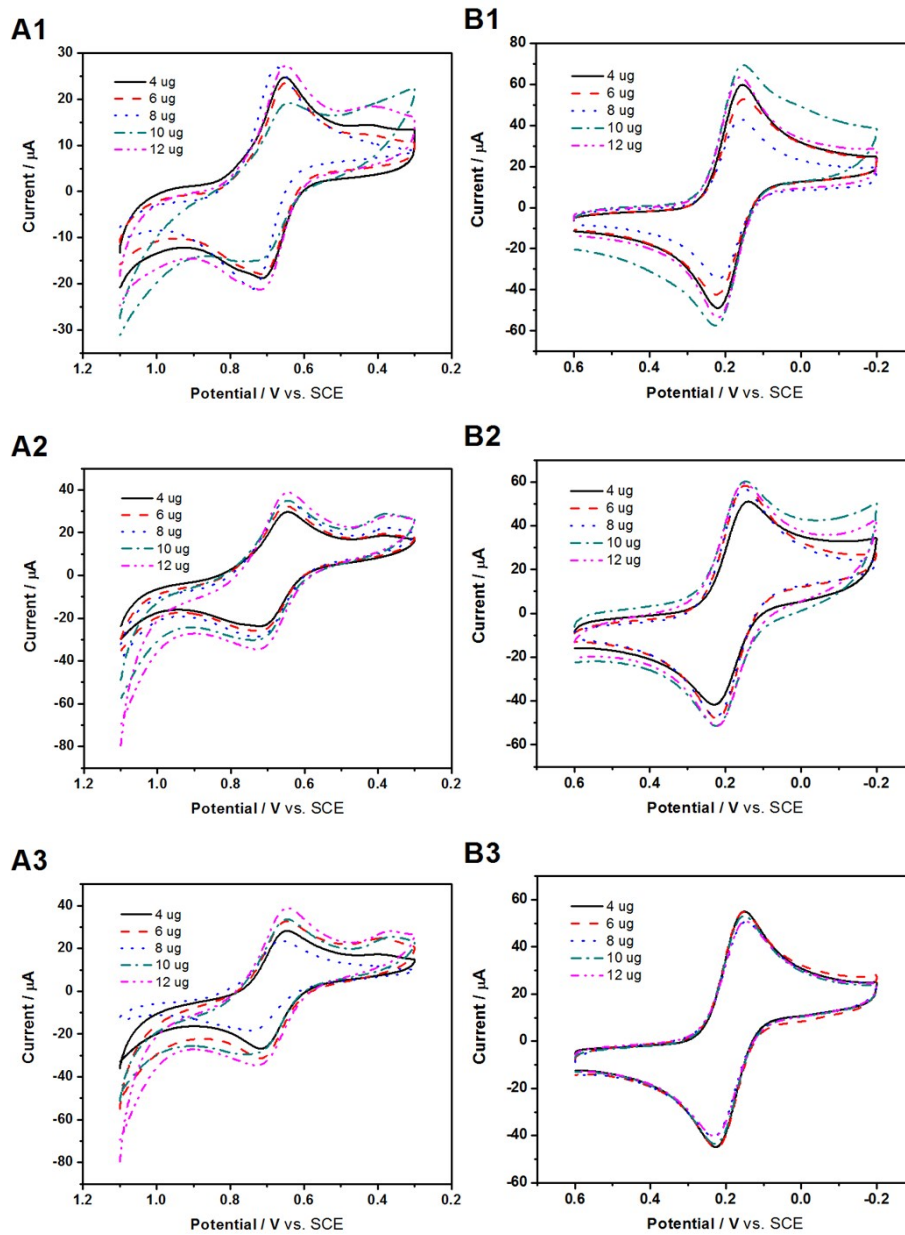


Fig. S4 CVs for different amounts at (A1, B1) Au/NCNT/GCE, (A2, B2) Au/PU-NCNT/GCE, and (A3, B3) Au/FU-NCNT/GCE. Condition: (A1–A3) 5.0 mM IrCl_6^{2-} in 0.1 M KCl, and (B1–B3) 5.0 mM $[\text{Fe}(\text{CN})_6]^{3-}$ in 0.1 M KCl, scan rate: $100 \text{ mV} \cdot \text{s}^{-1}$.

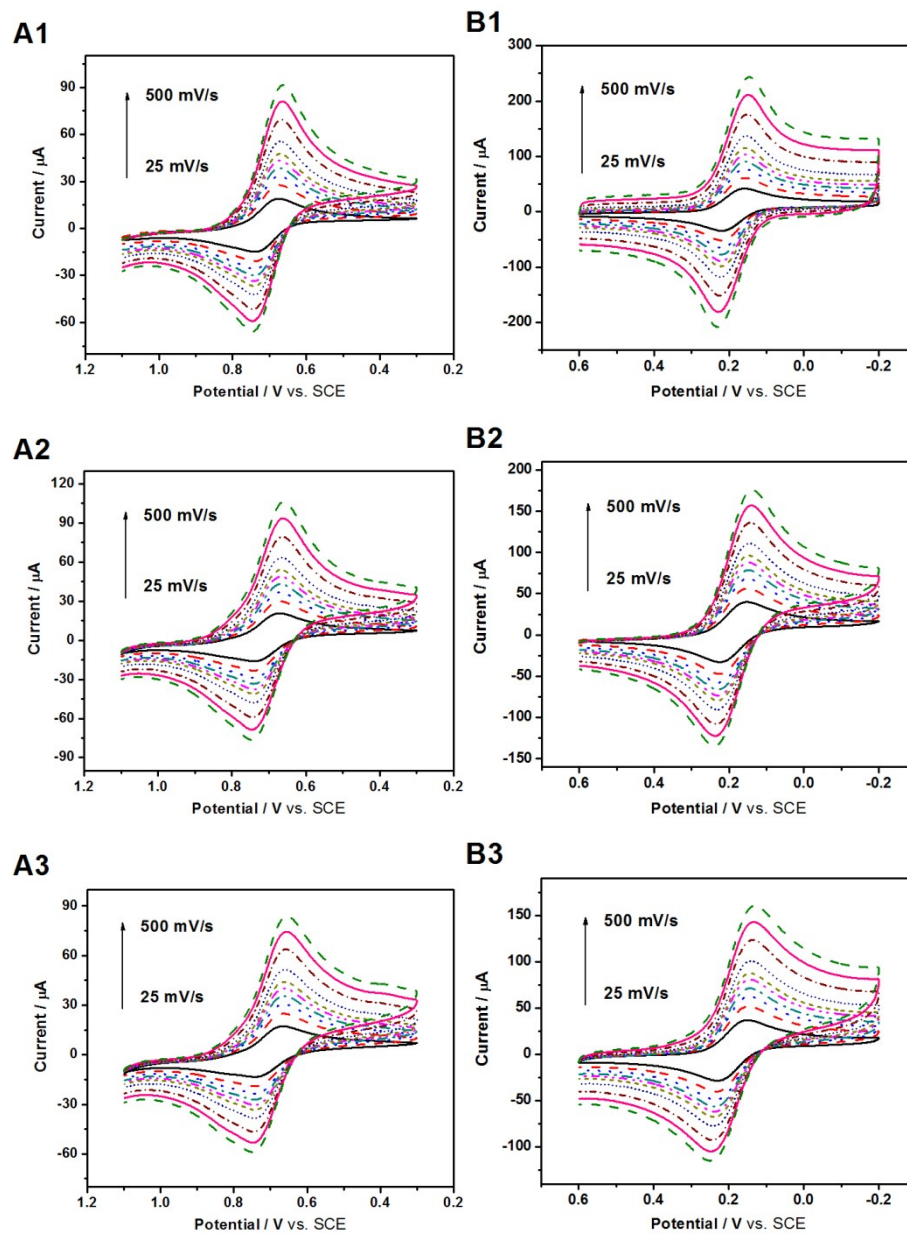


Fig. S5 CVs recorded at (A1, B1) Au/NCNT/GCE, (A2, B2) Au/PU-NCNT/GCE, and (A3, B3) Au/FU-NCNT/GCE in (A1–A3) 5.0 mM IrCl_6^{2-} in 0.1 M KCl, and (B1–B3) 5.0 mM $[\text{Fe}(\text{CN})_6]^{3-}$ in 0.1 M KCl at various scan rates: 25, 50, 75, 100, 125, 150, 200, 300, 400, and $500 \text{ mV} \cdot \text{s}^{-1}$.

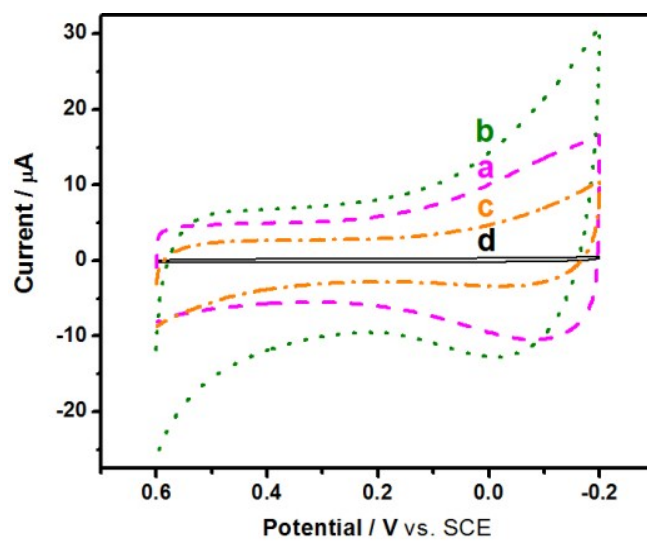


Fig. S6 (a) Au/NCNT/GCE, (b) Au/PU-NCNT/GCE, (c) Au/FU-NCNT/GCE and (d) bare GCE: CVs for 0.1 M PBS (pH 7.4). Scan rate: 100 mV·s⁻¹.

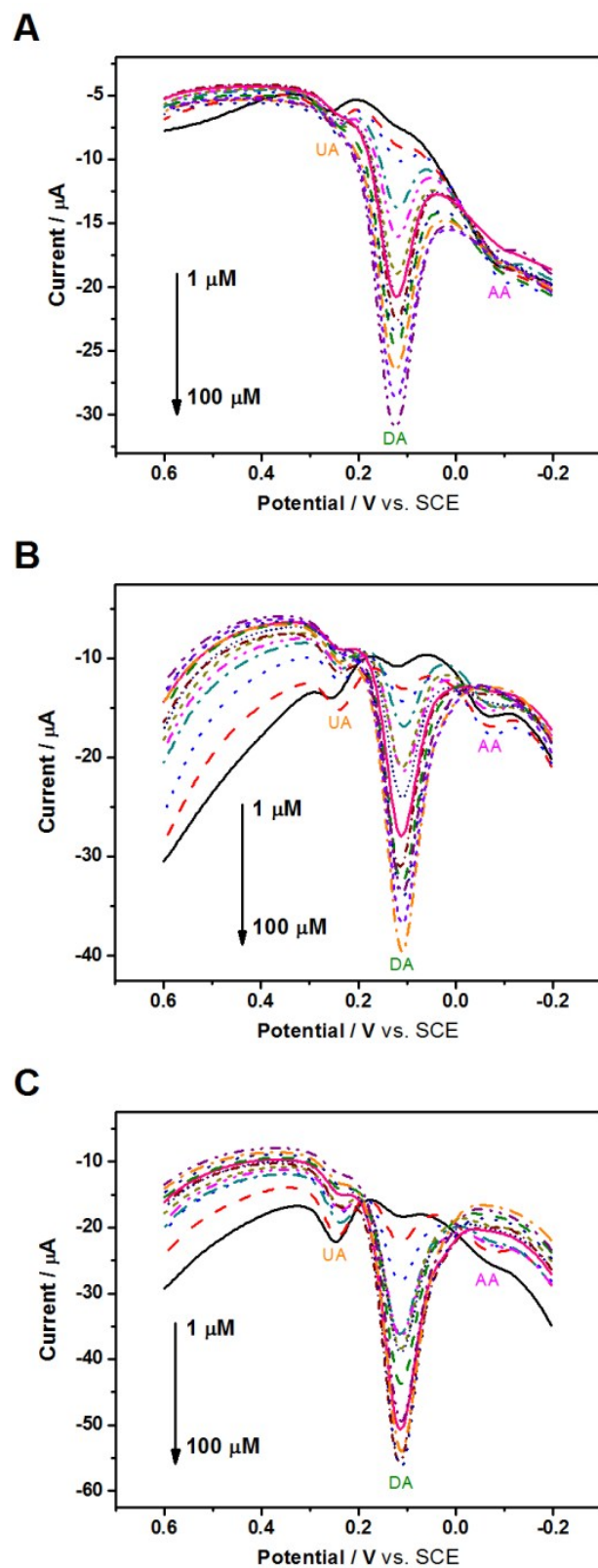


Fig. S7 DPVs of 1, 2, 5, 10, 15, 20, 30, 40, 50, 60, 70, 80, 90, 100 μM DA at (A) Au/NCNT/GCE, (B) Au/PU-NCNT/GCE, and (C) Au/FU-NCNT/GCE in the presence of 500 μM AA and 10 μM UA in 0.1 M PBS (pH 7.0). DPV, pulse period, 0.2 s; amplitude, 50 mV.

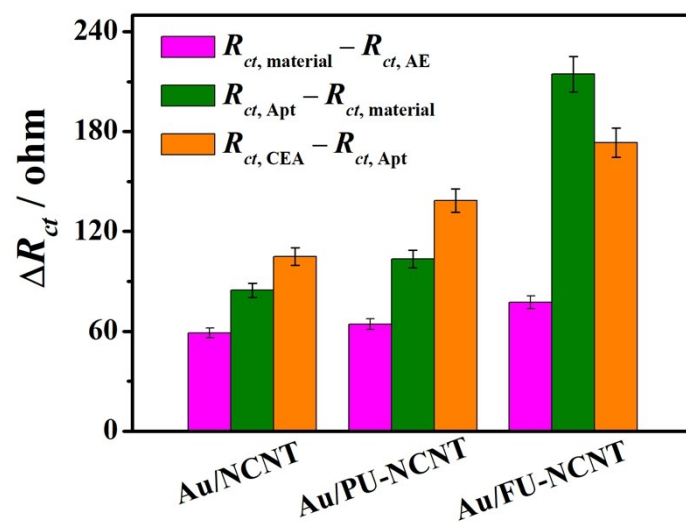


Fig. S8 Differences in ΔR_{ct} values at each stage for the CEA detection using the developed aptasensors based on Au/NCNT, Au/PU-NCNT, and Au/FU-NCNT.